Indian J. Phys. **75B** (1), 5– 10 (2001)

I J P B
an international journal

Cosmic ray energy spectrum above 10^{17} eV observed at Gauhati University mini array

T Bezboruah[1,*], K Boruah[2] and P K Boruah[3]

[1]Department of Electronics Science, Gauhati University, Guwahati-781 014, Assam, India

[2]Department of Physics, Guahati University, Guwahati-781 014, Assam, India

[3]Department of USIC, Gauhati University, Guwahati-781 014, Assam, India

E-mail bezboruah T @ caltiger.com

Received 21 March 2000, accepted 30 October 2000

Abstract The Gauhati University mini array of eight plastic scintillator of carpet area 2 m^2 has been operated since September 1996. The array detects giant Extensive Air Shower (EAS) by the method of time spread measurement of secondary particles. All the eight detectors are connected to a data acquisition system capable of recording arrival time spread of secondary particles upto 2.5 μS. Fast electronic circuits are employed to measure the density of shower particles as well as their arrival time spread with a resolution of 10 nS. We have reanalyzed the data recorded by the array during September 1996 to April 1999. The reanalysis shows marked improvement in the slope of the energy spectrum above 10^{17} eV. The best fitted differential energy spectrum observed by the mini array is $J(E) = 10^{25.38} \times E^{-3.04\pm.06}$ m^{-2} sr^{-1} s^{-1} eV^{-1}

Keywords UHE cosmic rays, extensive air showers, energy spectrum

PACS Nos. 96.40.De, 98.70.Sa, 96.40.Pq

1. Introduction

Every well-determined feature of the cosmic ray energy spectrum will have considerable impact on theories of the origin, acceleration, and propagation of cosmic rays. Particle accelerators at present, can provide particles upto a maximum energy of ~10^{14} eV. But in cosmic rays, particles beyond 10^{20} eV are available. Ultra High Energy (UHE) cosmic rays have gained importance as a result of highest energy events above 10^{20} eV being recorded by a number of research groups. According to the theory of Greisen cutoff, no primary cosmic ray particle should exceed energy of 10^{20} eV. Therefore study of such events with enough statistics is important for astrophysical purpose of origin. A giant extensive air shower can be conventionally detected using a large number of ground based detectors covering a wide area (several km^2). As suggested by Linsley [1], this can be done by a low cost method requiring a few closely packed detectors capable of measuring arrival time spread of individual shower particles. The idea has been pursued by us and a mini array detector has been installed in the Physics Department, Gauhati University. This detector array is specially designed to measure, both the charge particle density and their arrival time at the detector level. This paper presents the characteristics of the energy spectrum derived from the collected data by the present experimental setup.

2. The experiment

2.1. The technique

The Linsley effect is the increase in spread of arrival time distribution in a particle sample from a given shower with increasing distance from the shower centre. Thus, the measured time spread of particles striking localised detector system gives an estimate of the distance (r) to the shower axis. The number of particles give the measure of the local particle density (ρ). The shower size (N) is estimated from the assumed lateral distribution function and primary energy (E) is derived from the same.

Figure 1 shows the experimental arrangement of the detector system. The signals from the eight detectors are amplified and then carried to the control room *via* co-axial

*Corresponding Author

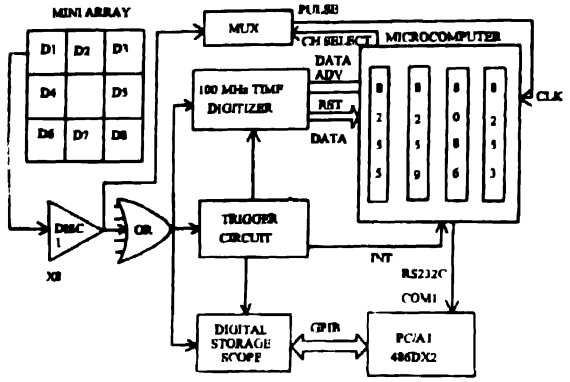

Figure 1. Block diagram of the experimental setup

cables (Type : RG58U). In the control room, all the eight signals are discriminated to provide corresponding logic signals. The discriminated output is then individually shaped into narrow pulses of 20 nS width and OR'ed together to give a serial pulse train. The serial pulse train is then branched into the time digitizer, the oscilloscope (Tektronix, TDS520, 500 MHz, 500 M Samples per sec) and the trigger unit. The trigger circuit senses the incoming pulse train and generates the necessary trigger pulse. Once triggered, the number of detector pulses and their relative time positions are stored in the time digitizer and the scope. The microprocessor (μP, 8086) stores the data from the time digitizer in RAM and transmits the data to the computer *via* serial port. The pulse waveform is recorded by the scope and is transferred to the PC (486DX2) *via* GPIB interface. The microprocessor also monitors the status of the detectors at a predetermined interval and also handles the recording and transfer of data of each event to the PC *via* RS232 interface. The details about the data acquisition system is presented elsewhere [2,3]

2.2. The detectors

Each detector unit consists of one fast photomultiplier tube (EMI 9807B), a plastic scintillator block of size . 50 × 50 × 5 cm^3 having polyvinyltolune base, a pre-amplifier unit and a light tight enclosure. Resolution of the scintillator is 20% with decay time of 4 nS, light output 50% that of anthracene and maximum wavelength of emission 4340 Å.

The count rate of the each of the detector is ~56.84 ± 0.987 Hz. The error is σ = 23.8. Omni directional pulse height distribution shows single particle peaks around 75 mV. Discriminator biases are set below this level. The relative time delays due to cable length and electronics are adjusted to zero by adding required extra lengths of cables. The minimum energy of particles detected by the detectors is about 100 MeV.

2.3. Calibration of the detectors

The integral cosmic ray flux of the secondary charged particles is, $F = 1.8 \times 10^{-2}$ m^{-2} s^{-1} and thus the number of charged particles crossing the scintillator block of area 0.25 m^2 is 45/s. Therefore, the single particle rate for one channel of the detector array can be considerd as 45 Hz. The calibration of the detector for single particle pulse height is done by using a standard single channel analyser (ECIL, SC604B) and a counter. All the eight discriminator biases are adjusted at the individual single particle level. The expected event trigger rate for the experiment is of the order of 10/day ($10^{17} < E < 10^{20}$ eV). The chance rate for the present setup for 3 particles with individual count rate of ~50 Hz is calculated to be 0.067/day [4].

2.4 Criterion for trigger

The purpose of the mini array is to scan the largest possible area consistent with given uncertainty. Therefore, we need to work with showers whose centres can fall upto a maximum distance determined by the minimum detected particle number that gives a tolerably small uncertainty. Thus, we are dealing with events where it is a good approximation that multiparticle hits on a detector are unlikely *i.e.* the detectors are effectively single particle counters. The conditions for generating a trigger are :

1. A hardware trigger requiring : particle in the range 2 or above within the time window.
2. The minimum time spread between the particles must be 100 nS

3. Theoretical estimation

Linsley and Scarsi [5] derived the empirical formula relating the shower disc thickness σ (nS) to the core distance $r(m)$, using experimental data from Volcano Ranch Array obtained by averaging over many showers as

$$\sigma = Br^{\beta}, \tag{1}$$

where B = 0.0158 and β = 1.5 and are derived from the experimental data. The particle density distribution for large shower and large core distances (r > 1000 m) is given by [6]

$$\rho = CNr^{-n}, \tag{2}$$

where C = 853, N = size of the shower and n = 3.8.

The integral and differential shower size spectra [7] are

$$J(N) = DN^{-\gamma}, \; j(N) = -\gamma DN^{-\gamma-1}, \tag{3}$$

where the constants have values D = 318 and γ = 1.7.

From eqs. (1) and (2),

$$r_{min} = (\sigma_1 / B)^{1/\beta}, \tag{4}$$

$$r_{max} = (CN / \rho_1)^{1/n} \tag{5}$$

Numerical calculations give the expected rate of collection of data as function of ρ_1 and σ_1 as

$$F_I(>\sigma_1, \rho_1) = 9.07 \times 10^6 \rho_1^{-1.7} \sigma_1^m, \tag{6}$$

where $m = (2 - n\gamma)/\beta$.

The integral shower size spectrum for σ_1 = 100 nS and ρ_1 = 1.5/m^2 is derived as

$$F_I(>N) = 2.209 \times 10^{10} N^{-1.174} - 63.46.10^{12} N^{-1.7} \text{ per day.} \tag{7}$$

Finally, the primary energy corresponding to an event with estimated shower size N is derived from the measurements of giant Array of Yakutsk, in agreement with QGS Model [8]. The best fit relation is obtained as

$$E \text{ (in eV)} = 1.122 \times 10^{13} \times N^{0.56}. \quad (8)$$

4. Data selection criteria

Numerical calculations [4] show that for a given threshold density (ρ_1 = 1.5/m^2), the minimum detectable shower size increases and the shower rate decreases with increasing time spread. A mini array should be able to pick out the very few large air shower events from a swarm of irrelevant events including the counter noises, the background soft radiations and small air showers. In order to eliminate the large number of small air showers, a minimum time spread has to be assigned. For a mini array of 2 m^2 area, a minimum acceptable shower size of 7.5 × 10^6 requires a minimum time spread σ_1 = 100 nS In view of the small particle density encountered, each scintillator is not expected to receive more than one particle at a time from a shower.

5. The simulation method

Assuming a given threshold density (ρ_1 = 1.5/m^2) and shower front thickness (σ_1 = 100 nS), r_{min} is calculated using [eq (4)]. Now, for a given value of N, say 10^7, r_{max} is calculated using [(eq. 5)]. For a particular event, core distance 'r' is chosen at random from an uniform distribution between r_{min} and r_{max}. With this value of r, σ is calculated using [eq. (1)] and ρ is calculated using [eq. (2)]. Errors of $\sigma \pm 10$ nS are superposed by using Gaussian distribution (Box-Muller method) Let the simulated thickness be σ_0. ρ_0 is simulated from Poisson distribution with mean 2ρ using the code poidev [7]. Expected shower size N_e for a given event is calculated using the relation

$$N_e = \frac{\rho_0}{C} \quad \frac{\sigma_0}{B}^{2.533}$$

This process is repeated 100 times to get the distribution of N Results for $N = 10^7$, 10^8 and 10^9 are shown in Figures (2–4). These distributions give an estimate of the errors in the measurement of shower size as 43.4%, 34% and 36% respectively.

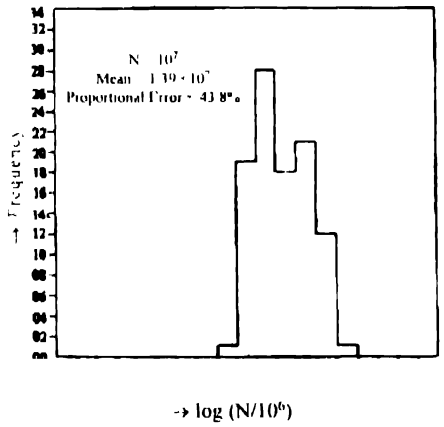

Figure 2. Artificial shower size spectrum from shower simulation with fixed shower size $N = 10^7$

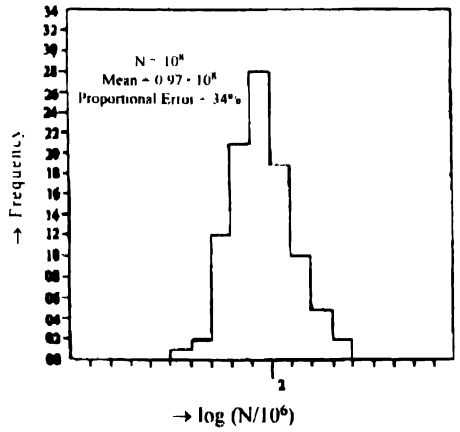

Figure 3. Artificial shower size spectrum from shower simulation with fixed shower size $N = 10^8$.

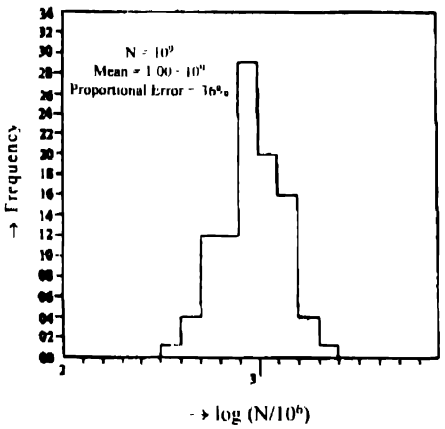

Figure 4. Artificial shower size spectrum from shower simulation with fixed shower size $N = 10^9$

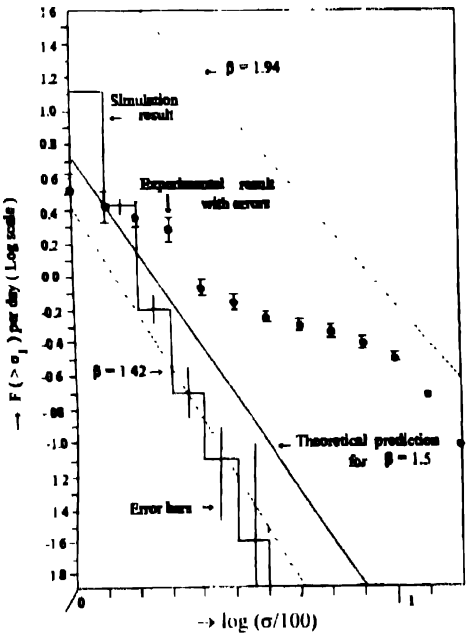

Figure 5. Integral shower rate spectrum with ρ = 1.5/m^2

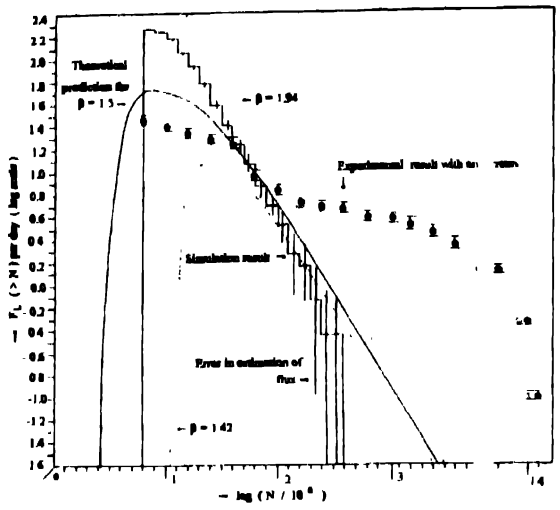

Figure 6. Integral shower size spectrum for $\rho = 1.5/m^2$

Artificial shower analysis is applied to estimate error by simulating N from the differential shower size spectrum [eq. (3)]. The resulting distribution (histogram) of shower disk thickness and shower size are shown in Figure 5 and Figure 6 respectively. The procedure for 100 simulations is repeated 30 times. In a given shower size bin (between N and $N + dN$) distribution of simulated flux is obtained from which mean and probable error are calculated. Results are shown in Figure 5 and Figure 6.

For the present experiment, primary energy is derived as a secondary parameter from the measurement of shower size N, using the relation [9]

$$E \text{ (in eV)} \quad 1.122 \times 10^{13} \times N^{0.56}.$$

Average percentage error in energy estimation is found to be ~22%.

6. Experimental results

Data have been collected during 1996 to 1999 for more than 1000 hours. Most of the data collected do not belong to true large shower events. The data are reduced by the selection process and by visual inspection. True large air shower events with a time spread of shower front $\sigma \geq 100$ nS and with local particle densities $\rho \geq 1.5/m^2$ are selected and analysed. They belong to shower of size $N \geq 7.5 \times 10^6$.

6.1. *Shower rate and size spectrum*

The integral shower rate spectra of the selected events as function of time spread are shown in Figure 5. The errors are estimated by considering the ± 10 nS instrumental error. The solid line is Linsley's theoretically predicted line [eq. (6)]. The upper and lower boundary lines (dashed) correspond to $\beta_{max} = 1.94$ and $\beta_{min} = 1.42$ as obtained from Linsley's later expression [10] for $10^{17} < E < 10^{20}$ eV and $r < 2$ km. From Figure 5, it is seen that for the three particle selection ($\rho = 1.5/m^2$), the experimental data are in reasonable agreement with the proposed power law upto $\sigma \leq 316$ nS. However, the experimental data are well within the predicted region bounded by the maximum and minimum lines.

In Figure 6, the integral shower size spectrum considering events with density $\rho_1 = 1.5/m^2$, is compared with theoretical prediction. The solid line corresponds to $\beta = 1.5$. The upper and lower dashed lines correspond to $\beta_{max} = 1.94$ and $\beta_{min} = 1.42$ respectively. The errors are calculated from the total recorded number of events. From the figure, it is seen that the experimental data are in reasonable agreement with the theoretical prediction upto shower size of 2.5×10^8.

6.2. *Energy spectrum* :

The energy spectrum derived from the mini array data exhibits remarkable structure. The differential energy spectrum considering the event above threshold ($\rho_1 \geq 1.5/m^2$), is shown in the Figure 7. The spectrum becomes steeper

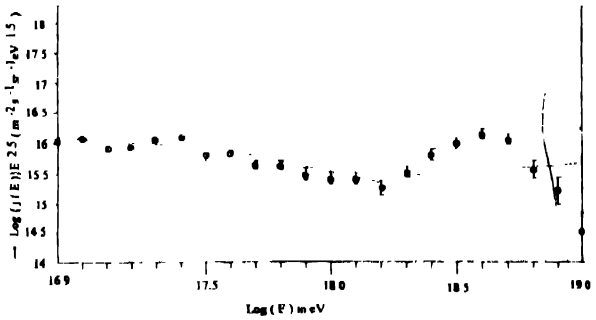

Figure 7. Mini array differential energy spectrum Points Data Dashed line best fit in each region Dotted line best fit upto $10^{18.2}$ eV

around $10^{17.6}$ eV and flattens around $10^{18.2}$ eV and forms a dip. We divide our mini array energy spectrum into three energy ranges and fit them to a power law in each region

Table 1. Normalization and spectral slope of $J(E)$

Energy range (eV)	Power index	χ^2	Log (normalization)	Normalized at (eV)
$10^{16.9} - 10^{19.0}$	−2.79 ± .04	37.08	−29.34	10^{18}
$10^{16.9} - 10^{17.6}$	−2.89 ± .12	27.50	−29.26	10^{18}
$10^{17.6} - 10^{18.2}$	−3.29 ± .09	12.54	−29.45	10^{18}
$10^{18.2} - 10^{19.0}$	−2.54 ± .06	35.55	−30.62	$10^{18.5}$
$10^{16.9} - 10^{18.5}$	−3.04 ± .06	28.40	−30.86	$10^{18.5}$

(Table 1). Table 1 also lists the overall fit regardless of the details of the spectrum, though the overall spectrum does not resemble a single power law. All the fits were done with the chi-squares fitting. A comparison has been done between the chi-squares fitting and maximum likelihood method. In general, the two methods show minor differences. For example, an overall mini array energy spectrum fitted with chi-squares fitting gives spectral slope of − 2.79 ± .05 while the maximum likelihood method gives a value of − 2.77. The spectral slope within the energy range $10^{17.6} - 10^{18.2}$ eV, is − 3.29 ± 0.09 from chi-squares fitting while maximum likelihood method gives − 3.27. The two numbers agree within the errors. To show the significance of the dip, the number of events expected from the overall fit (renormalized to the observed number of events at $10^{17.6}$ eV) are listed in

Table 2. Number of events expected and observed.

Energy bin $\{\log_{10}[E(eV)]\}$	Number of events expected from overall fit	number of events observed	Excess in σ from overall fit
16 9	100 36	130	02 96
17 0	139.57	203	05 36
17 1	207 27	133	−05 16
17.2	231.68	175	−03 72
17 3	231 06	383	10 00
17 4	261.85	394	08 17
17 5	196.09	146	−03 58
17 6	173 00	173	00 00
17 7	150 04	117	−02 70
17 8	128.53	106	01 99
17 9	109 11	063	−04 41
18 0	091.97	052	−04 17
18 1	077 13	049	−03 20
18 2	064 40	030	−04 29
18 3	053 62	046	−01 04
18 4	045 51	078	04 82
18 5	036.89	117	11 87
18 6	029 99	126	17 53
18 7	025 23	097	14 29
18 8	020 82	028	01 57
18 9	017 18	014	00 77
19 0	014 16	002	−03 23

Table 2 with the observed number of events. The expected number of events between $10^{17.6}$ eV and $10^{18.2}$ eV is 794 while the observed number is 590. The significance of the deficit is 7.52 σ. To show the significance of flattening above $10^{18.2}$ eV, we use the normalization and slope from the total fit upto $10^{18.3}$ eV. The total number of events observed above this energy is 538 while the expected number of events is 222. The significance of this excess is 21 18σ.

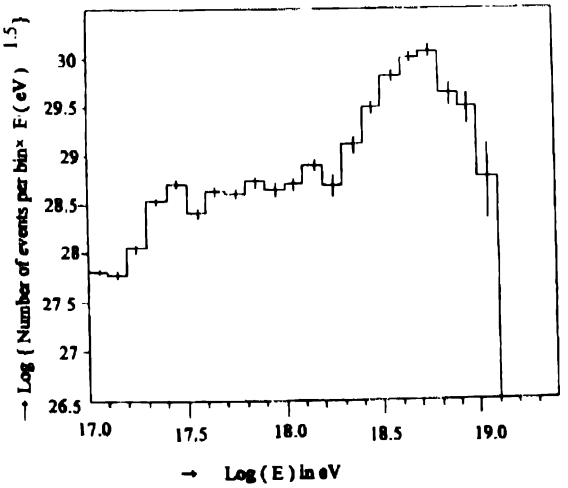

Figure 8. Mini array event distribution weighted by $E^{1.5}$ as function of energy

The existence of the dip can also be seen from analysing the raw data, by plotting event distribution weighted by $E^{1.5}$ as in Figure 8. From Figure 8 it is also seen that there is a dip formed around $10^{18.2}$ eV for the mini array energy spectrum.

7. Discussion and conclusion

In Figure 5 the result of the simulation for the distribution for artificial shower disk thickness, considering threshold density ρ = 1.5/m^2 and β = 1.5 is compared with the theoretical prediction and experimental result. In Figure 6, the result for the simulation of the artificial shower size spectrum for the same value of ρ and β is compared with theoretical prediction and experimental data. The simulation result for the artificial shower is in agreement with the theoretical prediction upto shower size of $N = 3.98 \times 10^8$. The experimental results agree with the theory upto 2.5×10^8 that corresponds to a primary energy of $10^{17.8}$ eV, above which there is a marked change in the slope of the shower size spectrum. The artificial shower simulation for the fixed shower of sizes 10^7, 10^8 and 10^9 predicts proportional errors of 43.8%, 34.0% and 36.0% respectively in the estimation of the shower size by using a mini array of area 2 m^2. The simulation gives an average error of 22% in the measurement of energy by the mini array. However, if we consider all the densities and shower front thicknesses above threshold then energy spectrum as shown in Figure 7, shows spectral changes similar to those observed by other large groups with

Table 3. Spectrum slopes

Experiment	Slope	Energy range (eV)
Haverah park	$3.14^{+0.05}_{-0.06}$	$10^{17.6}$ – $10^{20.0}$
Akeno	3.04 ± 0.04	$10^{15.7}$ – $10^{19.8}$
Akeno (Array 1)	3.24 ± 0.18	$10^{17.8}$ – $10^{18.8}$
Akeno (Array 20)	3.16 ± 0.08	$10^{18.3}$ – $10^{19.0}$
Yakutsk	3.23 ± 0.08	$10^{18.1}$ – $10^{19.0}$
Fly's eye (Mono)	3.07 ± 0.01	$10^{17.1}$ – $10^{19.6}$
Fly's eye (Stereo)	3.18 ± 0.02	$10^{17.1}$ – $10^{19.6}$
Mini array	3.04 ± 0.06	$10^{16.9}$ – $10^{18.3}$

overall slope of − 2.79. However, this slope is much lower than that calculated by others (Table 3) [11] and is due to the abnormally large number of events recorded by the mini array in the higher energy range (a significance of 21.18σ excess). This over estimation in the higher energy side may be due to inclusion of some delayed particles, which are not real part of the true shower front and thereby falsely increasing the thickness of the shower front. This gives an overestimation of the core distance, leading to higher energy estimation for a given particle density. Hence, we consider the overall spectrum for mini array upto $10^{18.3}$ eV with a slope of − 3 04 ± .06 which is in reasonable agreement with those calculated by the other groups. The differential energy spectrum corresponding to best fit (chi-squares fitting) in the energy region $10^{16.9}$ eV to $10^{18.3}$ eV is derived as :

$$j(E) = 10^{25.38} \times E^{-3.04 \pm .06}\ \mathrm{m^{-2}\ sr^{-1}\ s^{-1}\ eV^{-1}}.$$

A dip is clearly seen from the mini array energy spectrum as also observed by other groups. There is qualitative agreement in the spectral changes. Table 4 lists the slopes

Table 4. The dip

Experiment	Slope before the dip	First slope in the dip	Second slope in the dip
Akeno	3.02 ± 0.03 ($10^{15.7}$ – $10^{17.8}$)	3.16 ± 0.08 ($10^{17.8}$ – $10^{18.8}$)	2.80 ± 0.3 ($10^{18.8}$ – $10^{19.8}$)
Haverah park	3.01 ± 0.02 (10^{1} 10^{1}	3.24 ± 0.07 ($10^{17.6}$ – $10^{18.6}$)	$2.70^{+0.18}_{-0.17}$ ($> 10^{19}$)
Fly's eye (Stereo)	3.01 ± 0.06 ($10^{17.3}$ – $10^{17.6}$)	3.27 ± 0.02 ($10^{17.6}$ – $10^{18.5}$)	2.71 ± 0.10 ($10^{18.5}$ – $10^{19.0}$)
Mini array	2.85 ± 0.12 ($10^{16.9}$ – $10^{17.6}$)	3.29 ± 0.09 ($10^{17.6}$ – $10^{18.2}$)	2.54 ± 0.26 ($10^{18.2}$ – $10^{19.0}$)

over a relatively short energy range given by the experiments of various other groups of workers. The breaks are defined by each experiment independently. Each group has observed a significant deficit between 10^{18} eV and 10^{19}eV when compared to expectations of a continuation of the lower energy spectrum. However, the extension of the dip in case in mini array is much smaller than the others. The reanalysis shows a marked improvement in the slope of the energy spectrum in the lower energy region. The spectral break observed at $10^{17.6}$ eV, is in agreement with other world groups.

The spectral break at $10^{17.6}$ eV is due to a possible change in cosmic ray composition from predominantly light to predominantly heavy. The break at the position of dip ($10^{18.2}$ eV) indicates a possible change from galactic to extragalactic origin or possibility of a new cosmic ray source.

The overestimation of event rate at higher energy range may be due to inclusion of some delayed particles, small detector area and associated triggering criterion. By increasing the area of the mini array so that atleast 10 to 20 particles are detected per event, the unwanted events may be distinguished by careful investigations. It is therefore, proposed to extend the area of the mini array and to include one optical channel in order to collect genuine highest energy events.

Acknowledgment

This work has been supported by the grants from the Board of Research in Nuclear Sciences, Department of Atomic Energy, Government of India. The authors are thankful to Professor J Linsley Albuquerque, New Mexico, USA for his valuable suggestions during the work.

References

[1] J Linsley *J Phys* **G12** 51 (1986)

[2] T Bezboruah, K Boruah and P K Boruah *Nucl. Instrum. Meth Phys Res* **A410** 206 (1998)

[3] T Bezboruah, K Boruah and P K Boruah *Proc Symp on Advances in Nuclear and Allied Instrumentation* (Bombay) p 498 (1997)

[4] T Bezboruah, K Boruah and P K Boruah *Astro Part Physics* **11** 395 (1999)

[5] J Linsley and L Scarsi *Phys Rev Lett* **9** 123 (1962)

[6] T Hara, Y Hatano, N Hayashida, M Honda, F Ishikawa, T Kifune, M Nagano and M Teshima *Proc 18th Int Cosmic Rays Conf* (Bangalore) **vol. 11** p 276 (1983)

[7] W H Press, S A Teukolsky, W T Vellerling and Brain P Flannery *Numerical Recipes in Fortran* 2nd edn (Cambridge Cambridge University Press) p 279, p 284 (1994)

[8] A M Hillas *Phys Rep* **20C** 79 (1975)

[9] B N Afanasiev, M N Dyakonov, V P Egorova, S P Knurenko, V A Kolosov, S I Nikolsky and I Ye Sleptsov *Proc. 25th Int Cosmic Rays Conf* (Durban) **vol. 6** p 229 (1997)

[10] W S Li, P H Ng, and L K Ng *Proc 20th Int Cosmic Rays Conf* (Moscow) **Vol. 6** p 424 (1987)

[11] D J Bird, S C Corbato, H Y Dai, B R Dawson, J W Elbert, B L Emerson, K D Green, M A Huang, D B Kieda, M Luo, S Ko, C G Larsen, E C Loh, M H Salamon, J D Smith, P Sokolsky, P Sommers, J K K Tang and S B Thomas *Astrophys J.* **424** 491 (1994)